Core-Shell Ag@SiO2 Nanoparticles Concentrated on a Micro/Nanofluidic Device for Surface Plasmon Resonance-Enhanced Fluorescent Detection of Highly Reactive Oxygen Species

ARTICLE *in* ANALYTICAL CHEMISTRY · FEBRUARY 2014

Impact Factor: 5.64 · DOI: 10.1021/ac4037075 · Source: PubMed

7 AUTHORS, INCLUDING:

Xing-Hua Xia
Nanjing University
224 PUBLICATIONS **8,596** CITATIONS

SEE PROFILE

analytical chemistry

Article

pubs.acs.org/ac

Core–Shell Ag@SiO_2 Nanoparticles Concentrated on a Micro/Nanofluidic Device for Surface Plasmon Resonance-Enhanced Fluorescent Detection of Highly Reactive Oxygen Species

Huai-Song Wang,[†] Chen Wang,[†] Ya-Kai He,[†] Fang-Nan Xiao,[†] Wen-Jing Bao,[†] Xing-Hua Xia,*[,†] and Guo-Jun Zhou*[,‡]

[†]State Key Laboratory of Analytical Chemistry for Life Science, School of Chemistry and Chemical Engineering, Nanjing University, Nanjing 210093, China

[‡]Research Center of Zhejiang Tobacco Industry Company Limited, KeHai Road 118, Hangzhou 310024, China

Supporting Information

ABSTRACT: A micro/nanofluidic device integrating a nanochannel in a microfluidic chip was developed for sensitive fluorescent determination of highly reactive oxygen species (hROS) enhanced by surface plasmon resonance-enhanced fluorescence (SPREF). The nanochannel was simply fabricated by polyaniline nanostructures modified on a glass slide. Core–shell Ag@SiO_2 nanoparticles were concentrated in front of the nanochannel for fluorescence enhancement based on the SPREF effect. As a demonstration, hROS in the mainstream of cigarette smoke (CS) were detected by the present micro/nanofluidic device. The fluorescent probe for trapping hROS in puffs of CS employed a microcolumn that was loaded with a composite of DNA (conjugated fluorophores, FAM) and Au membrane (coated on cellulose acetate). With a laser-induced fluorescence detection device, hROS was determined on the basis of the amount of FAM groups generated by DNA cleavage. With the optimization of the trapping efficiency, we detected about 4.91 pmol of hROS/puff in the mainstream CS. This micro/nanofluidic-SPREF system promises a simple, rapid, and highly sensitive approach for determination of hROS in CS and other practical systems.

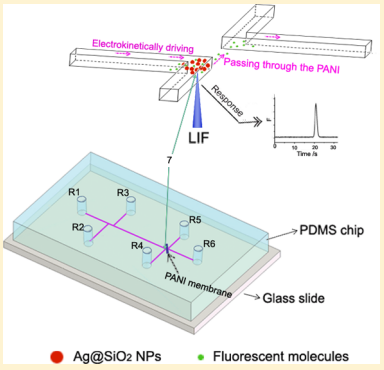

The miniaturized architecture of microfluidic system has provided a number of distinct advantages to chemical and biological analysis, such as advanced system integration and reduced volumes of samples and analytes.[1,2] For detecting the minute amount of analytes in the microchannel, highly sensitive detection methods have to be employed. Fluorescence-based sensors, especially laser-induced fluorescence (LIF), have been broadly applied in microfluidic analysis systems due to their high sensitivity, accuracy, and fairly good selectivity. For enhancing the fluorescence signal and reducing the background level, various LIF detection methods have been developed and successfully used in microfluidic chip-based analysis systems. One approach is to properly design the optical arrangements, such as confocal LIF, diode LIF, and orthogonal arrangements to reduce the scattered excitation light.[3−5] Another way to improve the fluorescence intensity is accomplished by nanostructure modification at the detection point of the microchannel, that is, the grating structures fabricated on quartz surfaces for surface-plasmon-enhanced fluorescence detection.[6,7] However, these methods usually need precise optical instruments or careful control of the spatial position of the micro- or nanostructure in the microfluidic chip, which limits their wider application.

Recently, surface plasmon resonance-enhanced fluorescence (SPREF) of core–shell metallic nanoparticles has been successfully used to increase the fluorescence intensity and improve the sensitivity of fluorescent detection. This SPREF phenomenon can be generated when fluorophores are in close proximity to the metal nanoparticle (i.e., gold or silver) surface, within a few nanometers. Upon irradiation with visible light, the localized surface plasmon resonance (LSPR) of metal nanoparticles will be excited, which results in an enhanced electromagnetic radiation field and thus increases the emission intensity of fluorophores in the vicinity of the nanoparticles.[8,9] The SPREF phenomenon is closely related to the distance between metallic nanoparticles and fluorophores. To easily control the nanometer distance, core–shell metallic nanoparticles have been used to enhance the fluorescence intensity and improve the sensitivity of fluorescence detection.[10−12] For example, core–shell Ag@SiO_2 nanoparticles (Ag@SiO_2 NPs) have been reported for ultrasensitive SPREF with numerous fluorophores.[13] The silica coating forms a controlled dielectric environment around the Ag NPs. By controlling the shell thickness of silica, the fluorescence enhancement can be optimized.

Received: November 15, 2013
Accepted: February 21, 2014
Published: February 21, 2014

Herein, we designed a microfluidic chip with integrated nanochannels to concentrate core−shell Ag@SiO_2 NPs, which can increase the fluorescence intensity of analytes via the SPREF effect. A polyaniline (PANI) membrane-modified glass slide and a poly(dimethylsiloxane) (PDMS) slab were integrated into the microfluidic chip to fabricate the micro/nanofluidic device (Figure 1).[14−16] The PANI membrane

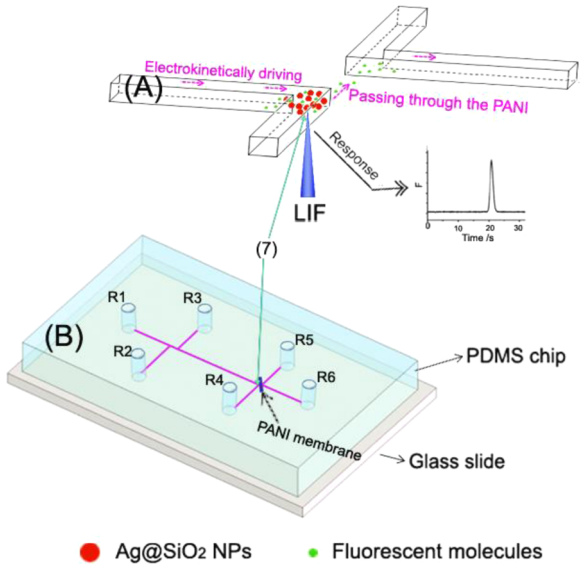

Figure 1. Schematic illustration of micro/nanofluidic device for Ag@SiO_2 NPs concentration. (R1, R3, R5, R6) Buffer reservoirs; (R2) sample reservoir; (R4) Ag@SiO_2 NPs reservoir; (7) laser-induced fluorescence detection point.

consists of highly dispersible PANI nanostructures, between which nanochannels are formed that can be effectively used to concentrate the Ag@SiO_2 NPs via size exclusion. Synthesis of the PANI membrane was based on the well-known chemical oxidative polymerization of aniline in a strongly acidic environment, with a simple "not shaken, not stirred" process.[16]

The micro/nanofluidic device, coupled with a LIF detection system, was used to detect highly reactive oxygen species (hROS) in cigarette smoke (CS) as a demonstration. hROS (e.g., $OH^•$, $ClO^•$, $^1O_2$) are implicated in a variety of human diseases including cancer. Numerous methods have been reported to detect and identify the very low concentrations of hROS in CS to understand the impact of hROS on biological, toxicological, and environmental processes.[17−20] Several fluorescence probes, such as dihydrorhodamine 6G (DHR 6G), dihydrorhodamine 123, and 2′,7′-dichlorofluorescein (DCF), have been applied for detection of ROS in CS.[21,22] These nonfluorescent compounds can be oxidized by ROS and become highly fluorescent dyes.

Even though the fluorescence-based method has shown convenient advantages for detecting ROS in CS, there are still numbers of cigarettes exhausted during the experimentation.[23,24] In order to reduce the sample and time consumption, the hROS in puffs of CS were trapped by a microcolumn and determined by use of the micro/nanofluidic device. The fluorescent probe for trapping the ROS from CS was immobilized in a composite of DNA (conjugated fluorophores) and Au membrane (coated on cellulose acetate, CA). In the composite, single-stranded DNA labeled with thiol group (at 3′-termini) and 6-carboxyfluorescein (6-FAM, at 5′-termini) was attached to the Au membrane via a covalent Au−S bond, where the Au was sputter-coated on CA beforehand. The single-stranded DNA is very reactive with hROS. This modified CA composite (FAM−DNA−Au/CA) was loaded in a microcolumn and used for probing hROS via detection of the free FAM groups generated from the cleavage of DNA oligomers. On the basis of the sensitive microfluidic system, we quantified the hROS in puffs of mainstream CS of selected cigarettes. This method gives fast time evaluation of oxidative activity of CS with low consumption of reagent, analysis time, and materials.

EXPERIMENTAL SECTION

Materials and Reagents. Ag@SiO_2 NPs with 80 nm core and 8 nm shell were prepared according to a previous report.[13] PDMS base and curing agent were purchased from Sylgard 184, Dow Corning (Midland, MI). The Research Cigarette (Liqun) was obtained from Zhejiang Tobacco Industry Co. Ltd. (Hangzhou, China). Scotch tape was purchased from 3M Company (Minneapolis, MN). Pluronic F127, tetraethoxysilane

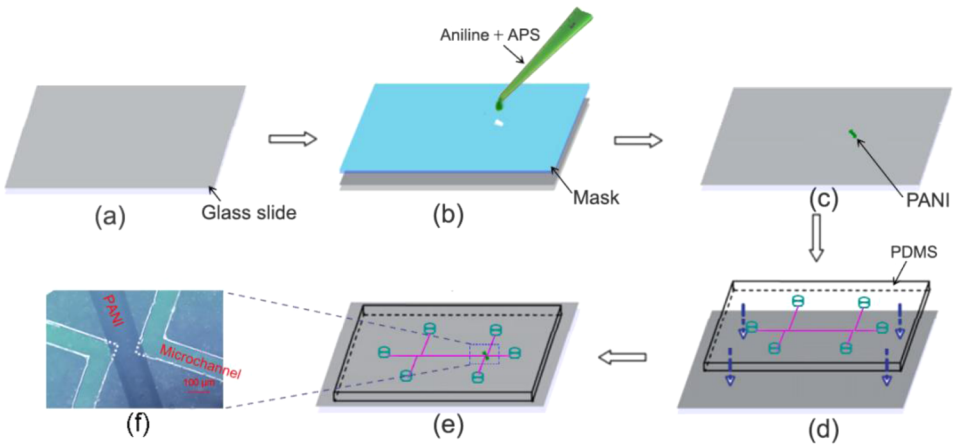

Figure 2. Schematic illustration of the micro/nanofluidic chip fabrication processes. (a) Glass slide; (b) Preparing of PANI membrane: One drop of aniline and APS mixture in HCl solution was added onto the glass slide covered with a mask, then the mixture was reacted with no shaken for 20 min; (c) Pattern transfer of the mask onto glass slide surface; (d) Sealing PDMS; (e) Formation of the final micro/nanofluidic chip. (f) Optical micrograph of the micro/nanofluidic circuit with an integrated nanostructured PANI.

dx.doi.org/10.1021/ac4037075 | Anal. Chem. 2014, 86, 3013−3019

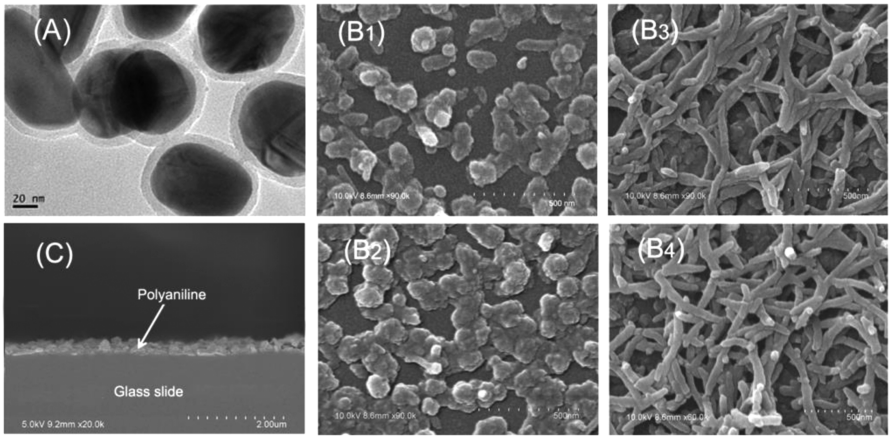

Figure 3. (A) TEM image of $Ag@SiO_2$ NPs. (B, C) SEM images of PANI-modified glass slides. PANI membrane was prepared with different reaction times (B_1, 10 min; B_2, 20 min; B_3, 30 min; B_4, 40 min). (C) Sectional SEM micrograph of the PANI membrane prepared as in panel B_2.

(TEOS), and 2′,7′-dichlorofluorescein (DCF) were purchased from Sigma−Aldrich (St. Louis, MO). Sodium citrate, silver nitrate, aniline, and ammonium persulfate were purchased from Nanjing Chemical Reagent Co. Ltd. (Nanjing, China). The single-stranded oligonucleotide used in this work (synthesis and purification by Shanghai Sangon, China) was derivatized with 3′-alkanethiol and 5′-FAM to give the following sequence: 3′-FAM-$(CH_2)_6$-CTCTCTCTC-$(CH_2)_3$-SH-5′ (FAM-DNA-SH). Borate buffer (pH 7.8, 20 mM) solution was used as the buffer system. All aqueous solutions were prepared from deionized water (18 MΩ·cm^{-1}, Purelab Classic, Pall Corp.). Liquid samples were filtered through a 0.22 μm syringe filter to remove particulates prior to use.

Instrumentation. Fluorescence detection was carried out by a laser-induced fluorescence (LIF) detection system as reported previously.[25] The excitation light comes from a 470 nm diode-pumped laser (Changchun New Industries Optoelectronics Tech Co., Changchun, China); the fluorescent light is detected by a photomultiplier tube after being transmitted through a 510 nm long-pass filter and a 525 nm band-pass filter (15-nm band-pass, Shenyang HB Optical Technology Co.). The morphology of $Ag@SiO_2$ NPs and PANI were characterized by transmission electron microscopy (TEM; JEM-200CX, Japan) and scanning electron microscopy (SEM; S-4800, Japan).

Fabrication of Micro/Nanofluidic Chip. The overall layout of the microfluidic device is represented in Figure 1B. The nanochannel on glass slide was fabricated by nanostructured PANI. Briefly, 0.65 M aniline was mixed rapidly with 0.16 M ammonium peroxydisulfate (APS) in 1.0 M HCl, and then one droplet of the mixture was dropped onto a dry glass slide. The reaction was performed at 25 °C for 20 min without mechanical disturbance. The PANI membrane was prepared after treatment by 3% ammonia solution for 0.5 h and then rinsed with water and ethanol to remove the unreacted reagent. The width and length of the membrane on the glass slide were framed by Scotch tape as a mask (see Figure 2b).

For fabrication of microchannels, a PDMS layer was directly cast over a silicon mold as previously described:[26] Sylgard 184 PDMS precursor (9.0 g) was mixed thoroughly with its cross-linking catalyst (1.0 g), and then 40 μL of saturated Pluronic F127 solution (~200 mg·mL^{-1}) was added. The precursor mixture was degassed under vacuum and poured on the silicon mold. After being polymerized at 80 °C for 40 min and cooled to room temperature, the PDMS slab was peeled from the mold. Finally, the PDMS slab with microchannels and reservoirs was reversibly sealed to the glass slide with PANI membrane to form a complete micro/nanofluidic chip. This assembly process is a "reversible" bonding between PDMS slab and glass slide.[27]

In this work, the length of the nanochannel, as well as the junction gap of the microchannel, was 100 μm. The dimensions of the microchannel were 18 μm high and 100 μm wide. The total length of the micro/nanofluidic chip (1−6) was 25 mm. Point 7 is the position for laser excitation and detection. The distance from reservoir 1 to the detection window was 15 mm.

Generation of Reactive Oxygen Species Trapping Agent. The FAM−DNA−Au/CA complex was prepared as the ROS trapping agent. Briefly, Au membrane was sputtered on CA (50 mg) for 100 s, and thenthis was added into 1.5 mL of phosphate buffer (10 mM, pH 7.4) containing 1.0 μM FAM−DNA−SH. The mixture was allowed to "age" for 20 h at room temperature. The unbound FAM−DNA−SH was removed by washing with phosphate buffer (10 mM, pH 7.4) and ethanol consecutively. The final prepared FAM−DNA−Au/CA composite was dried under vacuum.

Trapping Reactive Oxygen Species from Mainstream Cigarette Smoke. A microcolumn loaded with 5 mg of FAM−DNA−Au/CA complex was designed for hROS trapping in CS via solid-phase extraction (SPE). For sampling, the mainstream CS was flushed through the column via a puff protocol. By use of a 50 mL syringe, a 35 mL puff of 18 s duration was drawn from the cigarette for ROS trapping. The complete cycle was repeated every 20 s. Free FAM group, cleaved from the FAM−DNA−Au CA composite, was then obtained by elution from the SPE column by use of 1.0 mL borate buffer solution (pH 7.8, 20 mM) containing 15% ethanol.

Microchip Electrophoresis for Reactive Oxygen Species Quantitation. A LIF−microelectrophoresis detection system was used to quantify generated free FAM groups. The microchannels were sequentially flushed with water and borate buffer (pH 7.8, 20 mM) before use, each for 3 min. Reservoir 2 was filled with fluorescent sample, reservoir 4 was filled with $Ag@SiO_2$ NPs suspension [5% (w/w) in borate buffer solution], and remaining reservoirs were filled with buffer. Platinum electrodes were inserted into the individual reservoirs. A laboratory-made high-voltage power supply with voltage

dx.doi.org/10.1021/ac4037075 | Anal. Chem. 2014, 86, 3013−3019

ranging from 0 to 5000 V was used to apply electric fields to the microchannels through platinum electrodes placed in the reservoirs. The position of the microchip was fixed on a precise 3D adjustor and was adjusted to the focus point of the laser beam to illuminate the detection point on the microchannel with an effective separation length of 10 mm.

RESULTS AND DISCUSSION

Core–Shell Ag@SiO_2 Nanoparticle Selection. Ag NPs can dramatically change the optical properties of nearby fluorophores, including fluorescence quenching or enhancement. The strength of the quenching or enhancement can be influenced by many factors, such as the size and shape of the metal particles and especially the distance between fluorophore and metal.[10] Studies have shown that fluorescence quenching is usually observed if the fluorophore is located at a very short distance (<5 nm) from the metallic NP surface.[28−30] With increasing fluorophore–Ag NP distance, fluorescence enhancement (localized surface plasmon resonance-enhanced fluorescence or LSPREF phenomenon) can be observed. The optimal distance for Ag NP-induced LSPREF was reported to be about 8 nm.[31] For suitable LSPREF, core–shell Ag@SiO_2 NPs with 80 nm core and 8 nm shell were prepared according to a previous report.[13] A transmission electron micrograph of Ag@SiO_2 NPs is shown in Figure 3A. The dark Ag NPs covered with complete bright silica shells can be clearly observed. The average diameter of the Ag NPs is about 80 nm, and thickness of the bright shell of silica is about 8 nm. The silica shell can offer an optimal distance between Ag NPs and fluorophore for fluorescence enhancement.

Fabrication of Micro/Nanofluidic Chip. The fabrication process of micro/nanofluidic device is schematically shown in Figure 2. Briefly, there are three steps including (1) PANI membrane modification on the surface of a glass slide, (2) microchannel formation on a PDMS slab, and (3) final formation of a micro/nanofluidic chip.

Nanostructured PANI was used to fabricate the nanochannel in this study because of its simple synthesis, unique acid/base doping/dedoping chemistry, and excellent environmental stability. Furthermore, PANI nanostructures can facilitate the passage of charged analytes through the nanochannels, because PDMS and glass both can be negatively charged at near-neutral pH solution.[32] If the nanochannel is only formed by the PDMS thin-wall and glass substrate, the negatively charged analytes (DCF or FAM group) can be excluded from the entrance of the nanochannel and cannot easily pass through it.[33,34] In the present case, the nanochannel formed by PANI can avoid the charge-exclusion effect, because the secondary amido and phenyl groups in the wall of the nanochannel cannot be charged in the buffer solution (20 mM borate buffer, pH 7.8).

The highly dispersible PANI nanostructure was prepared on the surface of a glass slide with a simple "not shaken, not stirred" process.[14,16] We improved the polymerization proceeding in one drop of the reaction solution, from which the PANI nanostructures were synthesized by oxidative polymerization of aniline with APS in the presence of inorganic acid (HCl). Figure 3B shows SEM images of polyaniline aggregates formed with different reaction times. Being polymerized at room temperature, there were some coral-like aggregates besides the fibrous nanostructures. From Figure 3panels B_1–B_4, granular solids were first formed on the surface of glass slide, then PANI nanofibers were gradually grown on these granular solids with increasing reaction time. Nanochannels are thus formed between the PANI nanostructures. As shown in Figure $3B_2$ at reaction time of 20 min, the average size of nanochannels was less than 100 nm, which is suitable for concentrating the Ag@SiO_2 NPs via size-exclusion effect. This reaction time of 20 min was used for fabricating the micro/nanofluidic device. In the present work, the thickness of the PANI membrane was about 400 nm (Figure 3C), the width 150 μm, and the length about 600 μm.

For preparation of the microfluidic chip, PDMS was used as the polymer material due to its good thermal and oxidative stability, optical transparency and ease of fabrication. But the hydrophobic property of PDMS may result in nonspecific adsorption of analytes. In order to fabricate a hydrophilic PDMS surface, a triblock copolymer (Pluronic F127) was selected and embedded in PDMS precursor before the microfluidic chip preparation.[35] The performance of the Pluronic F127-modified PDMS chip was evaluated by use of 2′,7′-dichlorofluorescein (DCF) as the model analyte. Compared with the native PDMS chip, Pluronic F127-modified PDMS chip can reduce the nonspecific adsorption of DCF sample, especially for the first sample plug. In Figure 4, it can be

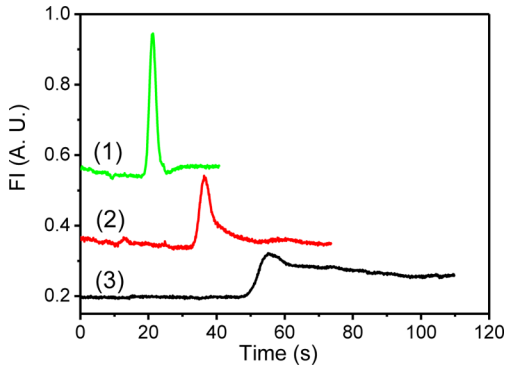

Figure 4. Electropherograms for the first sample plug of DCF solution on PDMS chip containing (1) 0.08% Pluronic F127 and (2) 0.04% Pluronic F127 and on (3) native PDMS chip. Gated sample injection was carried out by applying 500 V from R2 and R3 for 5 s. Working electrolyte, 20 mM borate buffer, pH 7.8; injection voltage, 200 V; separation voltage, 800 V.

observed that DCF is nearly irreversibly adsorbed on the native PDMS surface. Quantification of the following DCF samples will be affected by this residual DCF. On the Pluronic F127-modified PDMS chip, the irreversible adsorption decreases significantly with increasing Pluronic F127 content. On the PDMS chip containing 0.08% Pluronic F127, DCF displays a well-defined peak due to the significant hydrophilicity, which effectively eliminates nonspecific adsorption.

Fluorescence Enhancement of Ag@SiO_2 Nanoparticles. The SPREF effect of Ag@SiO_2 NPs concentrated in the micro/nanofluidic device was evaluated by analyzing DCF. DCF possesses similar fluorescence properties as FAM, and the sharp electropherogram peak can facilitate the evaluation of fluorescence enhancement. Before the evaluation, reservoir 2 was filled with DCF solution, reservoir 4 was filled with Ag@SiO_2 NPs suspended in 20 mM borate buffer (pH 7.8), and the remaining reservoirs were filled with borate buffer (see Figure 1). The evaluation progress is illustrated in Figure 5. First, DCF was analyzed by the micro/nanofluidic chip without Ag@SiO_2 NPs (panel I). Then 200 V potential was applied between reservoirs 4 and 5 for concentrating Ag@SiO_2 NPs at the

dx.doi.org/10.1021/ac4037075 | Anal. Chem. 2014, 86, 3013−3019

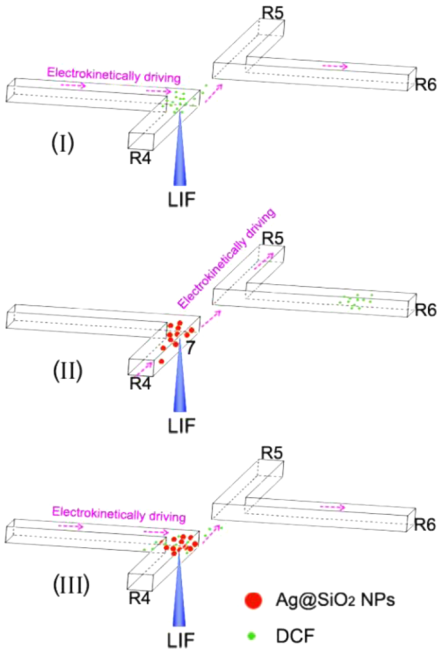

Figure 5. Evaluating fluorescence enhancement of $Ag@SiO_2$ NPs concentrated in micro/nanofluidic channels. (I) Electrophoresis of DCF in micro/nanofluidic channels; (II) concentrating $Ag@SiO_2$ NPs; (III) electrophoresis of DCF in micro/nanofluidic channels containing $Ag@SiO_2$ NPs.

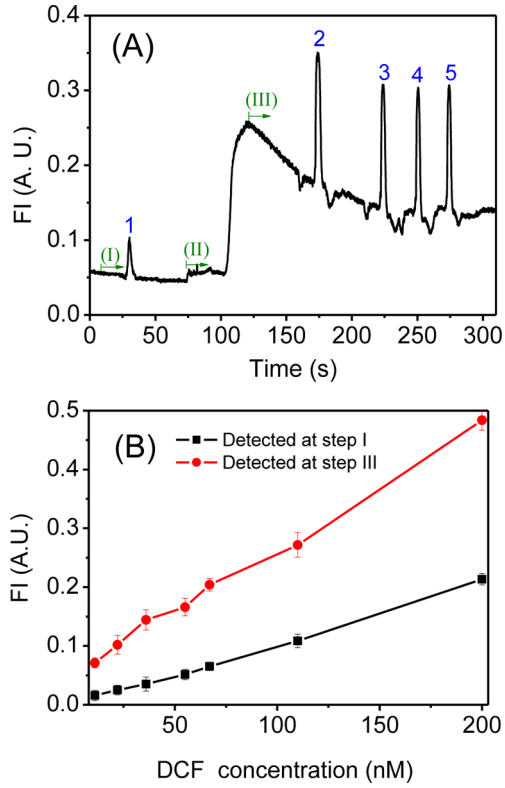

Figure 6. (A) Electropherograms for DCF solution (5.5×10^{-8} M) on micro/nanofluidic channels. (B) Standard curve of DCF. Error bars indicate standard deviations from three measurements for each concentration. Electrophoresis conditions were the same as described for Figure 4

detecting point 7 (panel II). Finally, DCF was analyzed by the micro/nanofluidic chip containing $Ag@SiO_2$ NPs, and enhanced DCF fluorescence can be observed (panel III).

A representative result for the evaluation progress is illustrated in Figure 6A. Peak 1 is the DCF signal detected in step I of Figure 5. Then the $Ag@SiO_2$ NPs were concentrated by the micro/nanofluidic chip for 50 s (from 75 to 125 s, step II). Peaks 2−5 are the DCF signals detected in step III after the completion of $Ag@SiO_2$ NP concentration. According to the repeated measurement of DCF (peaks 2−5), a reproducible result can be observed after the baseline has stabilized. When the DCF signals in steps I and III are compared, significant fluorescence enhancement is clearly observed. Similar fluorescence enhancement ability can also be achieved for FAM−DNA−SH on the micro/nanofluidic chip (Figure S1, Supporting Information). The SPREF effect of Ag core was further investigated by comparing the fluorescence spectra before and after removal of the Ag core (Figures S2 and S3, Supporting Information). It was found that, in the presence of Ag core, the fluorescence intensity of FAM−DNA−SH increased with increasing $Ag@SiO_2$ concentration.

It has been reported that the core−shell metallic nanoparticles were used to provide fluorescence enhancement from severalfold to about 100-fold, especially when the fluorophore was deposited on the shell surface either chemically or by vacuum deposition.[36,37] In this study, the SPREF effect can be observed when DCF was close to $Ag@SiO_2$ NPs during electrophoresis. Given that only a portion of DCF molecules have the chance to be in close proximity to Ag nanoparticles within a few nanometers, the fluorescence enhancement factor is thus not as higher as those reported. According to the standard curve of DCF at steps I and III (Figure 6B), the fluorescence signal of DCF is increased about 3-fold from 20 to 200 nM.

Probe Selection. In this work, cellulose acetate (CA) was used as the substrate to fabricate the fluorescent probe. As a cigarette filter, CA is thermotolerant, tough, low-cost, and easy to obtain. After the Au membrane was coated on CA by sputtering, FAM−DNA−SH was covalently attached on the surface of Au/CA via S−Au bond. The prepared FAM−DNA−Au/CA reacts with hROS, such as $OH^{\bullet}$, ClO^-, and $ONOO^-$, resulting in cleavage and strand breakage in the single-stranded DNA.[38,39] The free FAM groups can be eluted from CA and quantified by the micro/nanofluidic chip to evaluate the activity of hROS. Figure 7 illustrates the process for preparation of FAM−DNA−Au/CA and reaction with hROS. The amount of FAM groups grafted on FAM−DNA−Au/CA is detected by reaction of FAM−DNA−Au/CA with excessive $OH^{\bullet}$ (generated by Fenton reaction).[38] We detected 18.6 pmol/mg FAM groups grafted on FAM−DNA−Au/CA.

Gas-Phase Trapping. Before gas-phase trapping, FAM−DNA−Au/CA was loaded into a polypropylene microcolumn (Figure S4A,B, Supporting Information). hROS was scavenged from mainstream CS by use of the device shown in Figure S4C (Supporting Information). Mmainstream CS was sampled by the puffing method, which approximates the average puffing pattern of humans. The standard condition of one-puff method involves drawing 35 mL of smoke within 2 s duration every 10−20 s. In order to allow the hROS to fully react with FAM−DNA−Au/CA, we improved the puff condition that was drawing 35 mL of smoke within 18 s duration every 20 s for sample preparation. The final smoke samples for micro/nanofluidic chip determination were prepared with different numbers of puffs.

dx.doi.org/10.1021/ac4037075 | Anal. Chem. 2014, 86, 3013−3019

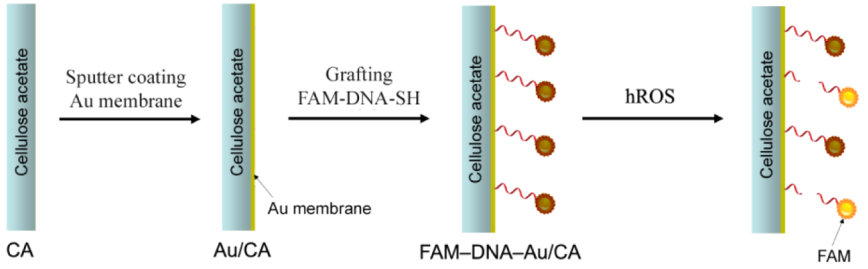

Figure 7. Preparation of FAM–DNA–Au/CA and reaction of FAM–DNA–Au/CA with hROS.

Quantitation of Reactive Oxygen Species in Cigarette Smoke. After trapping of hROS in CS by use of the microcolumn, the generated free FAM groups were eluted and detected by the micro/nanofluidic chip LIF detection system. According to Figure 8A, the fluorescence intensity changes increase linearly with numbers of puffs. The concentration of FAM groups is calculated from a standard curve obtained by plotting FAM–DNA–SH concentration versus fluorescent intensity. The linearity ranging from 4 to 64 nM is shown in Figure 8B. Concentrations of the generated FAM groups can be calculated from this standard curve. As reported before,[40−42] two molecules of hROS can induce the cleavage of a single-stranded DNA. Therefore, 24.55 pmol of hROS in five puffs (about 4.91 pmol of hROS/puff) for mainstream CS is calculated.

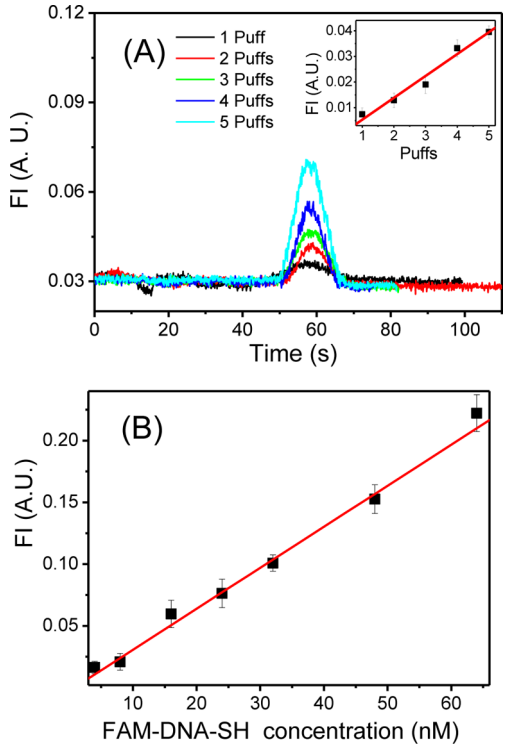

Figure 8. (A) Electropherograms for puff samples and (inset) fluorescence intensity per puff. Electrophoresis conditions were the same as described for Figure 4. (B) Standard curve of FAM–DNA–SH.

CONCLUSIONS

In the present work, a micro/nanofluidic device was designed and used to quantify hROS in the mainstream of CS based on the SPREF effect. The micro/nanofluidic device integratedh nanochannels, chip electrophoresis, and a LIF detector. The nanochannels were simply prepared by in situ polymerization of PANI membrane on glass slide. By use of this device, core–shell Ag@SiO_2 nanoparticles can be effectively concentrated in the front of the nanochannel via size-exclusion effect. The concentrated Ag@SiO_2 nanoparticles will effectively enhance the fluorescent intensity of fluorophores nearby. Thus, sensitive detection of oxidative activity of cigarette smoke has been achieved, based on cleavage of DNA oligomers labeled with fluorophores (FAM). This work promises a simple, rapid, and highly sensitive approach for determination of hROS in CS. We anticipate this micro/nanofluidic system will find wide applications for measuring aerosol oxidative activity.

ASSOCIATED CONTENT

Supporting Information

Four figures showing electropherograms for FAM-DNA-SH on micro/nanofluidic channels, TEM image of hollow SiO_2 spheres, fluorescence spectra of FAM-DNA-SH, and trapping of hROS in the mainstream of CS. This material is available free of charge via the Internet at http://pubs.acs.org.

AUTHOR INFORMATION

Corresponding Authors

*Fax +86-25-83685947; tel +86-25-83597436; e-mail xhxia@nju.edu.cn (X.-H. X.).

* E-mail guojunzhou@yahoo.com (G.-J. Z.).

Notes

The authors declare no competing financial interest.

ACKNOWLEDGMENTS

This work was supported by grants from the National 973 Basic Research Program (2012CB933800), National Natural Science Foundation of China (21035002, 21327902), National Science Fund for Creative Research Groups (21121091), Natural Science Foundation of Jiangsu Province (BK2010009), Tobacco Zhejiang Industrial Corp., Fundamental Research Funds for the Central Universities (20514340065), and China Postdoctoral Science Foundation (2013M531315).

REFERENCES

(1) Van den Berg, A.; Bergveld, P. *Lab Chip* **2006**, *6* (10), 1266–1273.

(2) Whitesides, G. M. *Nature* **2006**, *442* (7101), 368–373.

(3) Heus, F.; Giera, M.; de Kloe, G. E.; van Iperen, D.; Buijs, J.; Nahar, T. T.; Smit, A. B.; Lingeman, H.; de Esch, I. J. P.; Niessen, W. M. A.; Irth, H.; Kool, J. *Anal. Bioanal. Chem.* **2010**, *398* (7–8), 3023–3032.

(4) Fu, J. L.; Fang, Q.; Zhang, T.; Jin, X. H.; Fang, Z. L. *Anal. Chem.* **2006**, *78* (11), 3827–3834.

(5) Tawa, K.; Cui, X.; Kintaka, K.; Nishii, J.; Morigaki, K. *J. Photochem. Photobiol., A* **2011**, *221* (2−3), 261−267.
(6) Malic, L.; Veres, T.; Tabrizian, M. *Biosens. Bioelectron.* **2011**, *26* (5), 2053−2059.
(7) Cui, X.; Tawa, K.; Hori, H.; Nishii, J. *Adv. Funct. Mater.* **2010**, *20* (4), 546−553.
(8) Acuna, G. P.; Moeller, F. M.; Holzmeister, P.; Beater, S.; Lalkens, B.; Tinnefeld, P. *Science* **2012**, *338* (6106), 506−510.
(9) Cosa, G. *Nat. Chem.* **2013**, *5* (3), 159−160.
(10) Reineck, P.; Gómez, D.; Ng, S. H.; Karg, M.; Bell, T.; Mulvaney, P.; Bach, U. *ACS Nano* **2013**, *7* (8), 6636−6648.
(11) Roy, S.; Dixit, C. K.; Woolley, R.; O'Kennedy, R.; McDonagh, C. *Nanotechnology* **2012**, *23* (32), No. 325603.
(12) Guerrero, A. R.; Aroca, R. F. *Angew. Chem., Int. Ed.* **2011**, *50* (3), 665−668.
(13) Aslan, K.; Wu, M.; Lakowicz, J. R.; Geddes, C. D. *J. Am. Chem. Soc.* **2007**, *129* (6), 1524−1525.
(14) Huang, J.; Virji, S.; Weiller, B. H.; Kaner, R. B. *J. Am. Chem. Soc.* **2002**, *125* (2), 314−315.
(15) Li, D.; Huang, J.; Kaner, R. B. *Acc. Chem. Res.* **2008**, *42* (1), 135−145.
(16) Li, D.; Kaner, R. B. *J. Am. Chem. Soc.* **2005**, *128* (3), 968−975.
(17) Finkel, T.; Holbrook, N. J. *Nature* **2000**, *408* (6809), 239−247.
(18) Bartalis, J.; Zhao, Y. L.; Flora, J. W.; Paine, J. B.; Wooten, J. B. *Anal. Chem.* **2008**, *81* (2), 631−641.
(19) Robinson, E. A.; Johnson, J. D. *Mini-Rev. Org. Chem.* **2011**, *8* (4), 401−411.
(20) Colombo, G.; Dalle Donne, I.; Orioli, M.; Giustarini, D.; Rossi, R.; Clerici, M.; Regazzoni, L.; Aldini, G.; Milzani, A.; Butterfield, D. A.; Gagliano, N. *Free Radical Biol. Med.* **2012**, *52* (9), 1584−1596.
(21) Wang, S.; Li, N.; Pan, W.; Tang, B. *TrAC, Trends Anal. Chem.* **2012**, *39* (0), 3−37.
(22) Chen, X.; Tian, X.; Shin, I.; Yoon, J. *Chem. Soc. Rev.* **2011**, *40* (9), 4783−4804.
(23) Bartalis, J.; Zhao, Y. L.; Flora, J. W.; Paine, J. B., III; Wooten, J. B. *Anal. Chem.* **2009**, *81* (2), 631−641.
(24) Ou, B. X.; Huang, D. J. *Anal. Chem.* **2006**, *78* (9), 3097−3103.
(25) Wang, C.; Ouyang, J.; Ye, D. K.; Xu, J. J.; Chen, H. Y.; Xia, X. H. *Lab Chip* **2012**, *12* (15), 2664−2671.
(26) Wang, C.; Ouyang, J.; Gao, H. L.; Chen, H. W.; Xu, J. J.; Xia, X. H.; Chen, H. Y. *Talanta* **2011**, *85* (1), 298−303.
(27) Wang, C.; Li, S. J.; Wu, Z. Q.; Xu, J. J.; Chen, H. Y.; Xia, X. H. *Lab Chip* **2010**, *10* (5), 639−646.
(28) Cheng, D.; Xu, Q. H. *Chem. Commun.* **2007**, *3*, 248−250.
(29) Lakowicz, J. R. *Anal. Biochem.* **2005**, *337* (2), 171−194.
(30) Tovmachenko, O. G.; Graf, C.; van den Heuvel, D. J.; van Blaaderen, A.; Gerritsen, H. C. *Adv. Mater.* **2006**, *18* (1), 91−95.
(31) Li, H.; Chen, C. Y.; Wei, X.; Qiang, W.; Li, Z.; Cheng, Q.; Xu, D. *Anal. Chem.* **2012**, *84* (20), 8656−8662.
(32) Kim, S. M.; Burns, M. A.; Hasselbrink, E. F. *Anal. Chem.* **2006**, *78* (14), 4779−4785.
(33) Yu, H.; Lu, Y.; Zhou, Y. G.; Wang, F. B.; He, F. Y.; Xia, X. H. *Lab Chip* **2008**, *8* (9), 1496−1501.
(34) Shen, M.; Yang, H.; Sivagnanam, V.; Gijs, M. A. M. *Anal. Chem.* **2010**, *82* (24), 9989−9997.
(35) Wu, Z.; Hjort, K. *Lab Chip* **2009**, *9* (11), 1500−1503.
(36) Corrigan, T. D.; Guo, S.; Phaneuf, R. J.; Szmacinski, H. *J. Fluoresc.* **2005**, *15* (5), 777−784.
(37) Malicka, J.; Gryczynski, I.; Lakowicz, J. R. *Anal. Chem.* **2003**, *75* (17), 4408−4414.
(38) Tang, H.; Zhang, N.; Chen, Z.; Xu, K.; Zhuo, L.; An, L.; Yang, G. *Chem.—Eur. J.* **2008**, *14* (2), 522−528.
(39) Huang, W. T.; Xie, W. Y.; Shi, Y.; Luo, H. Q.; Li, N. B. *J. Mater. Chem.* **2012**, *22* (4), 1477−1481.
(40) Balasubramanian, B.; Pogozelski, W. K.; Tullius, T. D. *Proc. Natl. Acad. Sci. U.S.A.* **1998**, *95* (17), 9738−9743.
(41) Malins, D. C.; Polissar, N. L.; Gunselman, S. J. *Proc. Natl. Acad. Sci. U.S.A.* **1996**, *93* (6), 2557−2563.
(42) Worth, L.; Frank, B. L.; Christner, D. F.; Absalon, M. J.; Stubbe, J.; Kozarich, J. W. *Biochemistry* **1993**, *32* (10), 2601−2609.